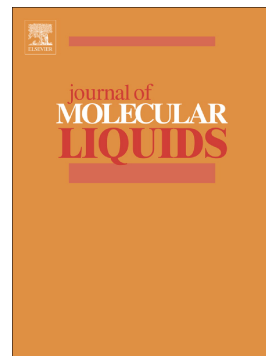


Accepted Manuscript

Compatibility of supported ionic liquid phase catalysts under ultrasonication

Megha Jagadale, Dolly Kale, Rajashri Salunkhe, Mohan Rajmane, Gajanan Rashinkar



PII: S0167-7322(18)30941-3
DOI: doi:[10.1016/j.molliq.2018.06.039](https://doi.org/10.1016/j.molliq.2018.06.039)
Reference: MOLLIQ 9237
To appear in: *Journal of Molecular Liquids*
Received date: 22 February 2018
Revised date: 5 June 2018
Accepted date: 10 June 2018

Please cite this article as: Megha Jagadale, Dolly Kale, Rajashri Salunkhe, Mohan Rajmane, Gajanan Rashinkar , Compatibility of supported ionic liquid phase catalysts under ultrasonication. Molliq (2017), doi:[10.1016/j.molliq.2018.06.039](https://doi.org/10.1016/j.molliq.2018.06.039)

This is a PDF file of an unedited manuscript that has been accepted for publication. As a service to our customers we are providing this early version of the manuscript. The manuscript will undergo copyediting, typesetting, and review of the resulting proof before it is published in its final form. Please note that during the production process errors may be discovered which could affect the content, and all legal disclaimers that apply to the journal pertain.

Graphical Abstract

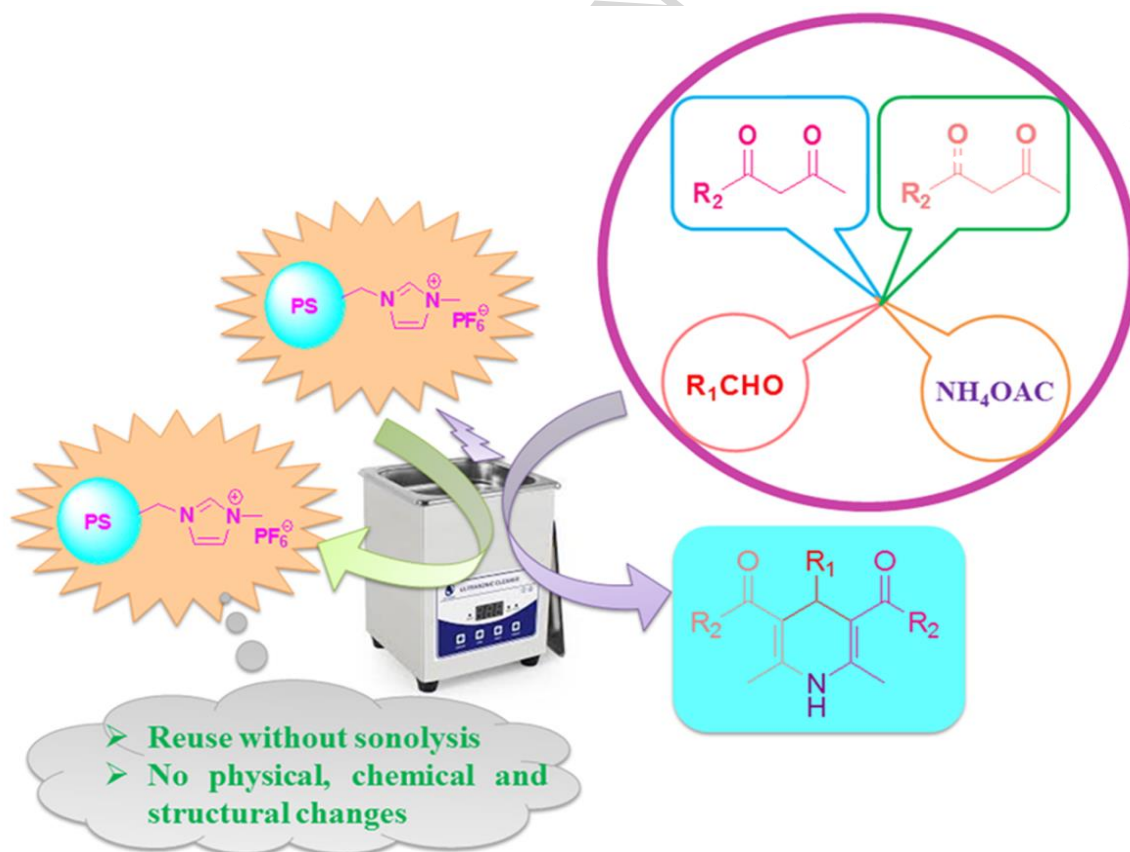
Compatibility of supported ionic liquid phase catalysts under ultrasonication

Megha Jagadale^a, Dolly Kale^a, Rajashri Salunkhe^a, Mohan Rajmane^b, Gajanan Rashinkar^{a*}^aDepartment of Chemistry, Shivaji University, Kolhapur, 416004, M.S., India^bSadguru Gadge Maharaj College, Karad, 415110, M.S., India

E-mail: gsr_chem@unishivaji.ac.in

*Corresponding author. Tel.: +91 231 260 9169; fax: +91 231 2692333.

Graphical abstract



Compatibility of supported ionic liquid phase catalysts under ultrasonicationMegha Jagadale^a, Dolly Kale^a, Rajashri Salunkhe^a, Mohan Rajmane^b, Gajanan Rashinkar^{a*}^aDepartment of Chemistry, Shivaji University, Kolhapur, 416004, M.S., India^bSadguru Gadge Maharaj College, Karad, 415110, M.S., India

E-mail: gsr_chem@unishivaji.ac.in

*Corresponding author. Tel.: +91 231 260 9169; fax: +91 231 2692333.

Abstract: Various supported ionic liquid phase (SILP) catalysts containing hexafluorophosphate anion have been prepared by covalent grafting of imidazolium ionic liquid in the matrix of cellulose, silica and Merrifield resin followed by anion metathesis reaction. The compatibility of SILP catalysts in the synthesis of 1,4-dihydropyridines under ultrasonication is investigated. The results revealed that SILP catalysts can be effectively used under ultrasonication without physical, chemical and structural changes as evidenced from various analytical techniques.

Keywords: Ionic Liquids; Supported ionic liquid phase; hexafluorophosphate anion; dihydropyridine; reusability.

1. Introduction

The advent of green chemistry principles has spurred unique interest in ultrasound assisted organic synthesis as it offers clean as well as energy conserving protocol [1]. It has potential benefits over conventional methods that include product selectivity, reduction in cost, energy and waste [2]. Mechanistic process of ultrasonication involves acoustic cavitation, which comprises generation, growth, oscillation and implosive collapse of bubbles inside the reaction medium leading to rate enhancement [3]. Recently, synergistic effect of Ionic Liquids (ILs) with

ultrasound has attracted considerable interest in the scientific community. Their combination is being increasingly exploited in diverse fields such as material science, organic synthesis, biomass processing, micro-extraction, waste water treatment and electrochemistry [4a]. Use of ILs with ultrasound as a non-conventional energy source offers diverse benefits in terms of energy economy, diminution in processing time and enhancement in mass transfer. Application of ILs as reaction media in sonochemical transformations is attributed to their negligible vapor pressure by the virtue of which efficiency of acoustic cavitation in bulk is altered noticeably that forces the substrates to collapse more violently, ultimately leading to acceleration in the rate of reactions [5]. However, despite these advantages the use of ILs under sonication has not progressed significantly as many of the ILs under ultrasound irradiation undergo decomposition into precursor azoles, alkyl halides, gaseous organic products and hydrocarbons [4]. In addition, physical effect of ultrasound on ILs leads to production of radicals at high frequency along with the rapid degradation. Moreover, the sonication of ILs leads to darkening of color as a function of time, which displays serious issues for industrial application as purification and decolorization steps of ILs result into poor E-factor [4a].

The concept of supported ionic liquid phase (SILP) catalysis involving immobilization of ILs onto surface of porous high-area support material has been recently introduced to circumvent the drawbacks associated with ILs. This new class of heterogenized version of ILs offer benefits chief of which is the ease of separation of catalyst simply by filtration as well as facilitating significant advances in selectivity, stability, recycling reproducibility and activity, decreases mass transfer limitation due to wide diffusion of reactants in highly viscous ILs [6]. Moreover, chemical transformations using SILP catalysts can be conducted under unusual conditions

employing fixed bed technology [7]. These advantageous properties have sparked significant interest in organic synthesis by employing SILP catalysts instead of ILs.

The scrutiny of literature reveals no report on the use as well as compatibility of SILP catalysts under ultrasonication. As the field of SILP catalysis is still in its infancy, we envisioned that such a study requires urgent attention as it can open new avenues for contemporary research in green chemistry. In continuation of our research in green chemistry [8], we herein report our pilot studies on the structural compatibility of SILP catalyst under ultrasonication.

2. Experimental

2.1 General remarks

All reactions were carried out under air atmosphere in dried glassware. Ultrasonication was performed in EN 50 US Enertech Make ultrasound cleaner with a frequency of 33 kHz and an output power of 120W. Infrared spectra were measured with a Perkin-Elmer one FT-IR spectrophotometer. The samples were examined as KBr discs~5% w/w. Raman spectroscopy was done by using Bruker FT-Raman (MultiRAM) spectrometer. The elemental compositions of material were analyzed by an energy-dispersive X-ray spectra (EDS) attached to the field emission scanning electron microscope (FE-SEM, Model Hitachi S 4800, Japan). ^1H NMR and ^{13}C NMR spectra were recorded on a Bruker AC (300 MHz for ^1H NMR and 75 MHz for ^{13}C NMR) spectrometer using CDCl_3 as solvent and tetramethylsilane (TMS) as an internal standard. Chemical shifts are expressed in δ parts per million (ppm) values and coupling constants are expressed in hertz (Hz). The CP-MAS ^{13}C NMR spectrum was recorded with a JEOL-ECX400 type FT-NMR spectrometer under prescribed operating condition. Mass spectra were recorded on a Shimadzu QP2010 GCMS. The morphology of materials were analysed by SEM using a JEOL model JSM with 5 kV and 20 kV accelerating voltage. Melting points were determined on

MEL-TEMP capillary melting point apparatus and are uncorrected. Aerogel silica, cellulose, alumina, Merrifield resin, potassium hexafluorophosphate and all other chemicals were obtained from local suppliers and used without further purification.

2.2 Preparation of chloropropyl aerogel silica (**3**)

A mixture of activated aerogel silica (**1**) (5.0 g) and 3-chloropropyltriethoxy silane (**2**) (5.0 mL, 22.7 mmol) in 25 mL of toluene was refluxed at 100 °C in an oil bath. After 24 h, reaction mixture was cooled and the product was filtered and repeatedly washed with toluene (3×5 mL) and dried under reduced pressure at 100 °C for 8 h to produce **3** (4.9 g).

2.3 Preparation of [SilImi]Cl (**5**)

A mixture of **3** (4g) and 1-*N*-methyl-imidazole (**4**; 5.0 mL, 8 mmol) in 25 mL of DMF was heated at 80 °C in an oil bath. After 72 h, the insoluble product was filtered, washed with DMF (3 x 50 mL), MeOH (3 x 50 mL), CH₂Cl₂ (3 x 50 mL) and dried under vacuum at 50 °C for 24 h to afford **5**. IR (KBr, thin film): $\nu = 3422, 2940, 2034, 1870, 1636, 1574, 1463, 1136, 806, 648, 621, 572, 465 \text{ cm}^{-1}$; Raman: $\nu = 3068, 2999, 2959, 2897, 2711, 2406, 1916, 1786, 1724, 1595, 1483, 1417, 1336, 1156, 1022, 893, 791, 680, 480 \text{ cm}^{-1}$; Elemental analysis observed: % C 8.34, % H 1.34, % N 2.07; Loading: 0.73 mmol imidazolium unit g⁻¹ of silica.

2.4 Preparation of [SilImi]PF₆ (**6**)

A mixture of **5** (3g) and 7% aqueous KPF₆ solution (25 mL) was vigorously stirred at ambient temperature. After 24 h, the insoluble product was filtered, washed with copious amount of water and dried under vacuum at 50 °C for 24 h to afford **6**. IR (KBr, thin film): $\nu = 3451, 2955, 2008, 1873, 1633, 1575, 1419, 1154, 841, 649, 622, 558, 489, 426, 408 \text{ cm}^{-1}$; Raman: $\nu = 3035, 2967, 2921, 2899, 2839, 2768, 2702, 2662, 2519, 2491, 1925, 1782, 1730, 1527, 1456, 1379, 1146, 1052, 787, 745, 648, 461 \text{ cm}^{-1}$; Elemental analysis observed: % Si 28.42, % O 45.10, % N 1.89,

% C 16.56, % P 1.21, % F 6.81; Loading: 0.40 mmol functional group g^{-1} of silica.

2.5 Preparation of Cell- Al_2O_3 composite (**8**)

Blend of microcrystalline cellulose (**7**, 15 g), aluminum chloride hexahydrate (15 g) in water (200 mL) was stirred for 12 h. The mixture was subsequently filtered and resultant solid was exposed to ammonia. Finally, it was washed with water and dried under vacuum at room temperature to get **8**. The amount of aluminum was determined by calcining 0.300 g of **8** to 600 °C for 8 h and the residue weighed as Al_2O_3 , which was found to be 3.24 wt%, corresponding to 0.67 mmol g^{-1} aluminum.

2.6 Preparation of chloropropyl cellulose (**9**)

A mixture of **8** (10.0 g) and (3-chloropropyl)triethoxysilane (**2**; 9.6 mL, 43.6 mmol) in 25 mL of toluene was refluxed in an oil bath. After 24 h, reaction mixture was cooled, the product was filtered and washed with toluene (3×5 mL) and dried under vacuum at room temperature for 8 h to produce **9**. IR (KBr, thin film): $\nu = 3366, 2898, 1623, 1427, 1335, 1204, 1160, 1109, 1056, 1032, 707, 667 \text{ cm}^{-1}$; Loading: 0.67 mmol functional group g^{-1} of cellulose.

2.7 Preparation of [CellIMi]Cl (**10**)

A mixture of **9** (7.0 g) and 1-*N*-methyl-imidazole (**4**; 8.84 mL, 14 mmol) in DMF (25 mL) was heated at 80 °C in an oil bath. After 72 h, the solid was filtered, washed with DMF (3×50 mL), MeOH (3×50 mL), CH_2Cl_2 (3×50 mL) and dried under vacuum at 50 °C for 24 h to afford **10**. IR (KBr, thin film): $\nu = 3346, 2902, 2129, 1642, 1574, 1371, 1317, 1281, 1245, 1061, 897, 665, 619, 579 \text{ cm}^{-1}$; Raman: $\nu = 3163, 3071, 2896, 2597, 2446, 2370, 2249, 1893, 1728, 1576, 1468, 1377, 1337, 1119, 1095, 785, 515 \text{ cm}^{-1}$; Elemental analysis observed: % C 39.78, % N 1.84, % H 5.96; Loading: 0.65 mmol imidazolium unit g^{-1} of cellulose.

2.8 Preparation of [CellImi]PF₆ (**11**)

A mixture of **10** (5.0 g) and 7% aqueous KPF₆ solution (40 mL) was stirred at room temperature for 24 h. Afterwards, the mixture was filtered and the residue was washed with water and dried under vacuum at 50 °C for 24 h to afford **11**. IR (KBr, thin film): $\nu = 3356, 2902, 2130, 1640, 1429, 1371, 1336, 1317, 1281, 1246, 1113, 1059, 837, 707, 665, 617, 599 \text{ cm}^{-1}$; Raman: $\nu = 3157, 2894, 2652, 2583, 2498, 2391, 2200, 2128, 1885, 1729, 1591, 1467, 1380, 1339, 1290, 1119, 1095, 777, 734, 617 \text{ cm}^{-1}$; Elemental analysis observed: % Si 0.44, % Al 0.49, % N 6.78, % C 61.71, % P 1.63, % F 9.43, % O 19.53; Loading: 0.54 mmol functional group g⁻¹ of cellulose.

2.9 Preparation of [MerImi]Cl (**13**)

A mixture of Merrifield resin (**12**; 1.0 g) and 1-*N*-methyl-imidazole (**4**; 1.26 mL, 2.0 mmol) in 15 mL of DMF was heated at 80 °C in an oil bath. After 72 h, the polymer was filtered, washed with DMF (3 × 20 mL), MeOH (3 × 20 mL), CH₂Cl₂ (3 × 20 mL) and dried under vacuum at 50 °C for 48 h to afford **13**. IR (KBr, thin film): $\nu = 3398, 3025, 2919, 2850, 1731, 1600, 1568, 1492, 1444, 1364, 1156, 904, 750, 691, 612 \text{ cm}^{-1}$; Raman: $\nu = 3054, 2904, 2852, 2404, 1815, 1601, 1449, 1332, 1185, 1155, 1029, 1000, 790, 619 \text{ cm}^{-1}$; Elemental analysis observed: % C 78.76, % H 7.30, % N 4.34; Loading: 1.55 mmol imidazolium unit g⁻¹ of resin.

2.10 Preparation of [MerImi]PF₆ (**14**)

[MerImi]Cl (**13**; 1.0 g) was suspended in 7% aqueous solution of KPF₆ (10 mL). The reaction mixture was stirred for 24 h at room temperature, Afterwards the polymer was filtered and washed with water and dried under vacuum at 50 °C for 24 h to afford **14**. IR (KBr, thin film): $\nu = 3398, 3025, 2919, 2850, 1731, 1600, 1568, 1492, 1444, 1364, 1156, 1019, 826, 750, 691, 612 \text{ cm}^{-1}$; Raman: $\nu = 3056, 2901, 2851, 2541, 2477, 2406, 2320, 2191, 2144, 2006, 1602, 1448,$

1325, 1186, 1078, 1028, 1000, 793, 780, 739, 619 cm^{-1} ; Elemental analysis observed: % C 75.20, % N 11.00, % P 1.92 and % F 11.88; Loading: 0.64 mmol functional group g^{-1} of resin.

2.11 General procedure for the synthesis of 1,4-dihydropyridines

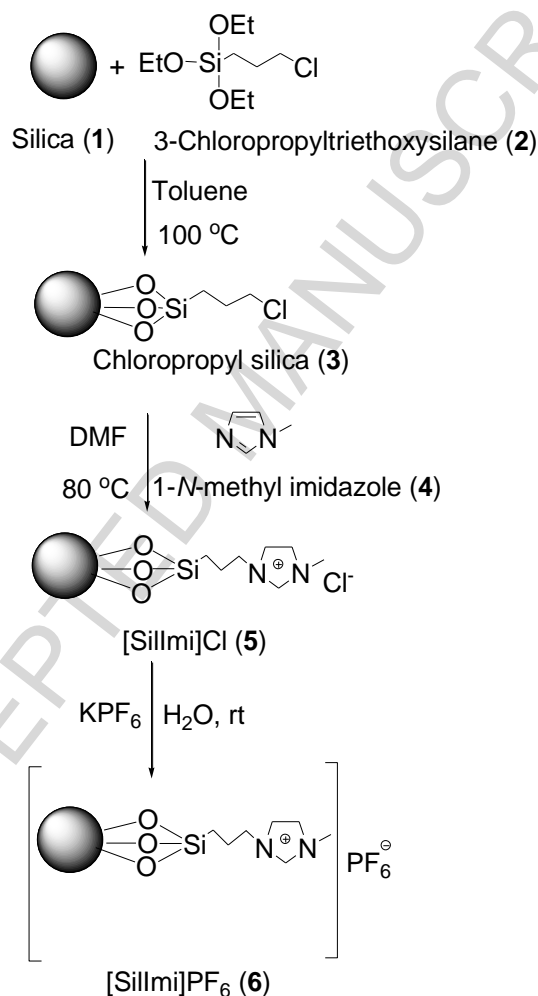
A mixture of aldehyde (**15**; 1.0 mmol), ethyl acetoacetate (**16**; 2.0 mmol), ammonium acetate (**17**; 1.0 mmol) and [MerImi]PF₆ (**14**; 100 mg) in ethanol (5 mL) was sonicated at ambient temperature. After completion of the reaction as monitored by TLC, the reaction mixture was filtered to remove insoluble catalyst. Evaporation of solvent in vacuo followed by column chromatography over silica gel using petroleum ether/ethyl acetate afforded pure 1,4-dihydropyridine derivatives.

3. Results and Discussion

The most striking approach for the synthesis of SILP catalysts involve covalent attachment of IL like units on high area porous support materials since it reduces probability of leaching. The commonly employed supports are those which are easily accessible, insoluble in common solvents, non-toxic, cost effective, biocompatible and have excellent thermal and chemical stability. In this regard, silica, cellulose and Merrifield resin have been widely used as supports in the synthesis of SILP catalysts [9]. This prompted us to employ silica, cellulose and Merrifield resin as supports in the synthesis of SILP catalysts in the present work. The SILP catalysts were synthesized by covalent attachment of imidazolium units containing hexafluorophosphate anion. Our interest in the incorporation of PF₆ as a counter anion is rationalized on the basis of wide applicability of ILs containing hexafluorophosphate anion in the organic synthesis [10].

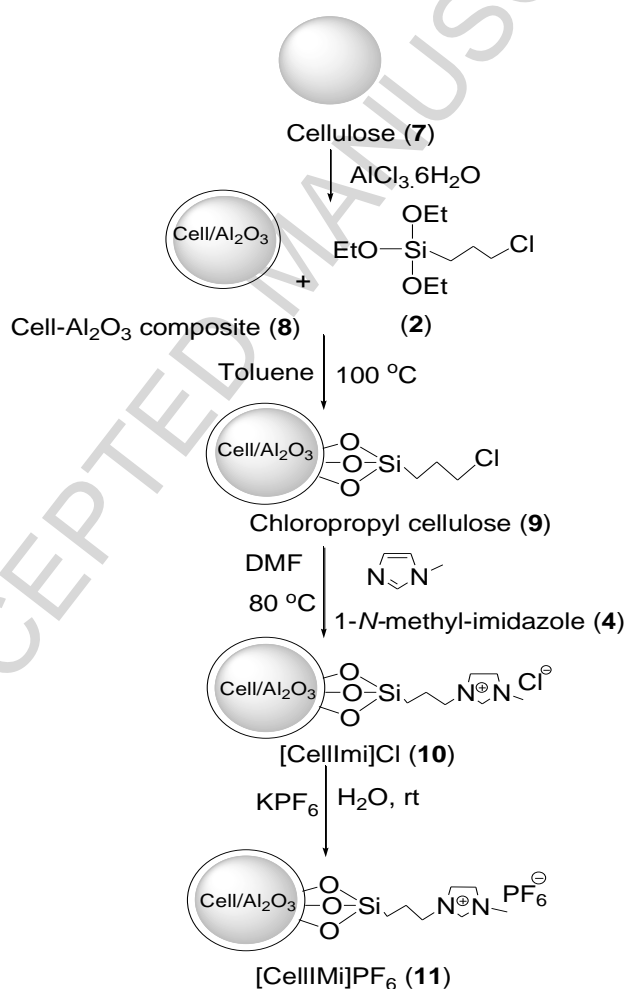
The synthesis of silica SILP catalyst is outlined in **Scheme 1a**. Initially, organofunctionalization of silica was achieved by reacting the activated silica (**1**) with (3-

chloropropyl)triethoxysilane (**2**) to yield chloropropyl silica (**3**). Synthetically active chloro group in **3** allowed installation of IL like unit in silica matrix *via* quaternization of 1-*N*-methyl imidazole (**4**) to produce heterogeneous azolium salt acronymed as [Sillmi]Cl (**5**). The anion metathesis reaction of **5** with aqueous potassium hexafluorophosphate solution resulted in the formation of desired silica SILP catalyst containing hexafluorophosphate anion acronymed as [Sillmi]PF₆ (**6**).



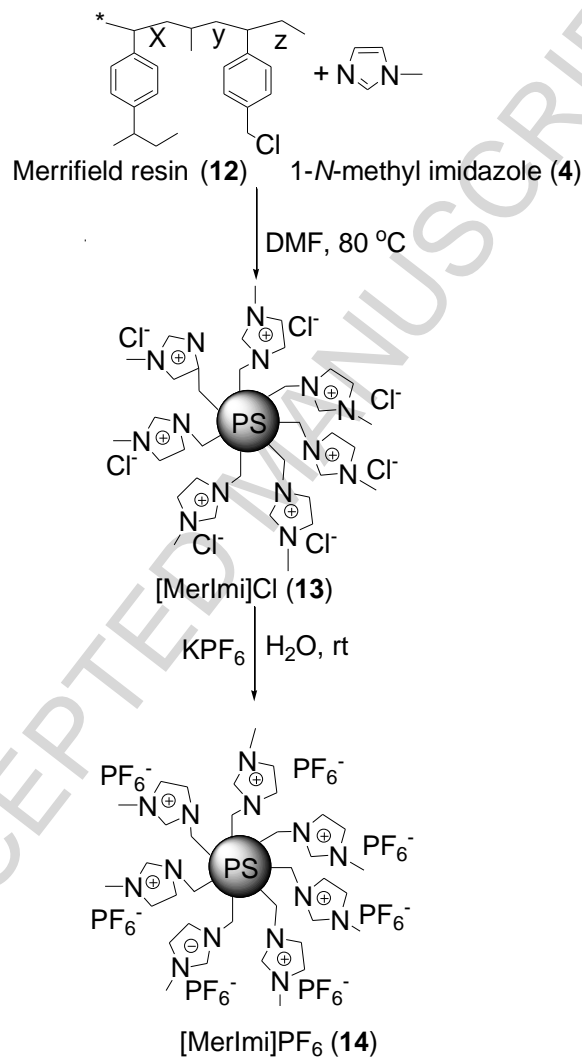
Scheme 1a. Synthesis of silica supported ionic liquid phase catalyst containing hexafluorophosphate anion, [Sillmi]PF₆ (**6**)

The preparation of cellulose SILP is summarized in **Scheme 1b**. Initially, Cell- Al_2O_3 composite (**8**) was prepared by uniform dispersal of alumina on the cellulose matrix (**7**). Reaction of Si-OEt group of (3-chloropropyl)triethoxysilane (**2**) with surface Al-OH groups of **8** allowed facile synthesis of chloropropyl cellulose (**9**). 1-*N*-methyl imidazole (**4**) was then grafted on **9** to afford SILP catalyst precursor acronymed as [CellImi]Cl (**10**). Finally, the anion metathesis reaction of **10** with aqueous potassium hexafluorophosphate solution yielded the desired cellulose SILP catalyst containing hexafluorophosphate anion acronymed as [CellImi]PF₆ (**11**).



Scheme 1b. Synthesis of cellulose supported ionic liquid phase catalyst containing hexafluorophosphate anion, [CellImi]PF₆ (**11**)

The synthesis of Merrifield resin SILP catalyst is depicted in **Scheme 1c**. Initially, 1-*N*-methyl imidazole (**4**) was covalently anchored on Merrifield resin (**12**) to yield heterogeneous azolium salt acronymed as [MerImi]Cl (**13**). The anion metathesis reaction of **13** with aqueous potassium hexafluorophosphate solution resulted in the desired Merrifield resin SILP catalyst containing hexafluorophosphate anion acronymed as [MerImi]PF₆ (**14**).



Scheme 1c. Synthesis of Merrifield resin supported ionic liquid phase catalyst containing hexafluorophosphate anion, [MerImi]PF₆ (**14**)

The successful synthesis of [SilImi]PF₆ (**6**), [CellImi]PF₆ (**11**), [MerImi]PF₆ (**14**) was confirmed by Fourier transform-Raman (FT-Raman), Fourier transform-infrared (FT-IR) and

cross-polarization magic angle spinning (CP-MAS) ^{13}C NMR spectroscopy. The FT-Raman analysis of **6**, **11**, **14** displayed characteristic peaks due to out-plane C-H bending vibrations of imidazolium ring [787 cm^{-1} for **6**, 777 cm^{-1} for **11**, 793 cm^{-1} for **14**], in-plane wagging vibrations of alkyl chain [1052 cm^{-1} for **6**, 1095 cm^{-1} for **11**, 1078 cm^{-1} for **14**], symmetrical stretching vibrations of alkyl chain [2899 cm^{-1} for **6**, 2894 cm^{-1} for **11**, 2901 cm^{-1} for **14**] and symmetric P-F stretching of PF_6 anion [745 cm^{-1} for **6**, 734 cm^{-1} for **11**, 739 cm^{-1} for **14**] supporting the formation of desired SILP catalysts. In addition, the FT-IR spectra exhibited typical peaks due to in-plane C-H deformation vibrations of imidazolium ring [1154 cm^{-1} for **6**, 1113 cm^{-1} for **11**, 1156 cm^{-1} for **14**], C-H bending vibrations of $-\text{CH}_3$ [1419 cm^{-1} for **6**, 1429 cm^{-1} for **11**, 1444 cm^{-1} for **14**], in-plane C-N stretching vibrations of imidazolium ring [1633 cm^{-1} for **6**, 1640 cm^{-1} for **11**, 1592 cm^{-1} for **14**] and the characteristic peaks of P-F stretching of PF_6 anion [841 cm^{-1} for **6**, 837 cm^{-1} for **11**, 826 cm^{-1} for **14**] suggesting the formation of desired SILP catalysts.

The formation of **14** was further corroborated by recording the CP-MAS ^{13}C NMR spectrum which demonstrated sharp peak at 41.0 ($-\text{CH}_3$ of imidazolium ring), 52.9 ($-\text{CH}_2$ group between imidazolium and benzene ring), 128.3, 137.1, 146.2 (imidazolium Cs), 120-146 (peaks due to C atoms of aromatic polystyrene framework overlapped with peaks of imidazolium Cs) confirming the proposed structure.

The quantification of IL like units was ascertained on the basis of EDX analysis. The loading of 0.40 mmol functional group g^{-1} of silica for **6**, 0.54 mmol functional group g^{-1} of cellulose for **11** and 0.64 mmol functional group g^{-1} of resin for **14** was observed.

The thermogravimetric analysis (TGA) of $[\text{SilImi}]\text{PF}_6$ (**6**), $[\text{CellImi}]\text{PF}_6$ (**11**) and $[\text{MerImi}]\text{PF}_6$ (**14**) is displayed in **Fig. 1-3**. The TGA curves of **6** and **11** displayed initial weight

loss of 2.55% (26-239 °C) and 5.17% (26-83 °C) due to desorption of physically adsorbed water. Additionally, two subsequent weight losses of 8.20% (239-251 °C) and 4.39% (251-304 °C) for [SiIImi]PF₆ (**6**) while 53.66% (195-390 °C) and 3.36% (390-400 °C) for [CellImi]PF₆ (**11**) were observed due to collective combustion of surface bound organic scaffolds. The decomposition of IL like unit resulted in further weight loss of 12.39% for [SiIImi]PF₆ and 21.81% for [CellImi]PF₆ (**11**). Finally, the large residual weight is ascribed to the formation of silica for [SiIImi]PF₆ (**6**) and decomposition of cellulose units through the formation of levoglucosan and other volatile compounds for [CellImi]PF₆ (**11**). TGA thermogram of [MerImi]PF₆ (**14**) displayed initial weight loss of 59.17% (248 °C to 464 °C) due to collective loss of organic moiety and IL like units confined on Merrifield resin. Second weight loss of 13.10% (464 °C to 592 °C) is ascribed to the decomposition of Merrifield resin backbone. Finally the residual weights correspond to formation of carbonaceous matter and generation of carbonates due to incomplete combustion of polymeric material.

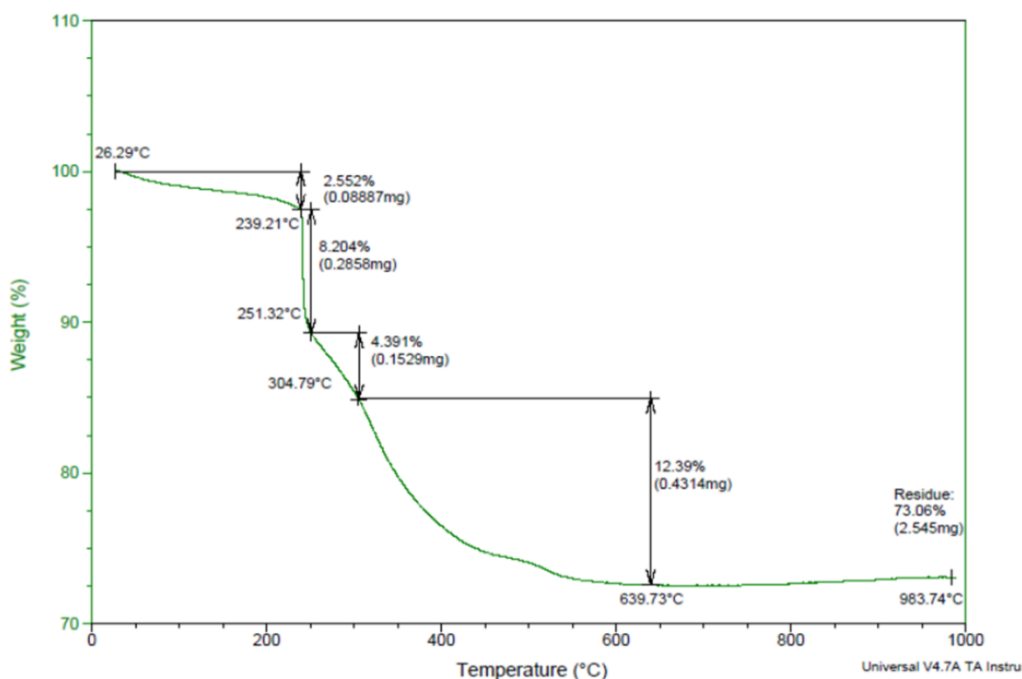


Fig. 1. Thermogravimetric analysis (TGA) curve of [SiIImi]PF₆ (**6**)

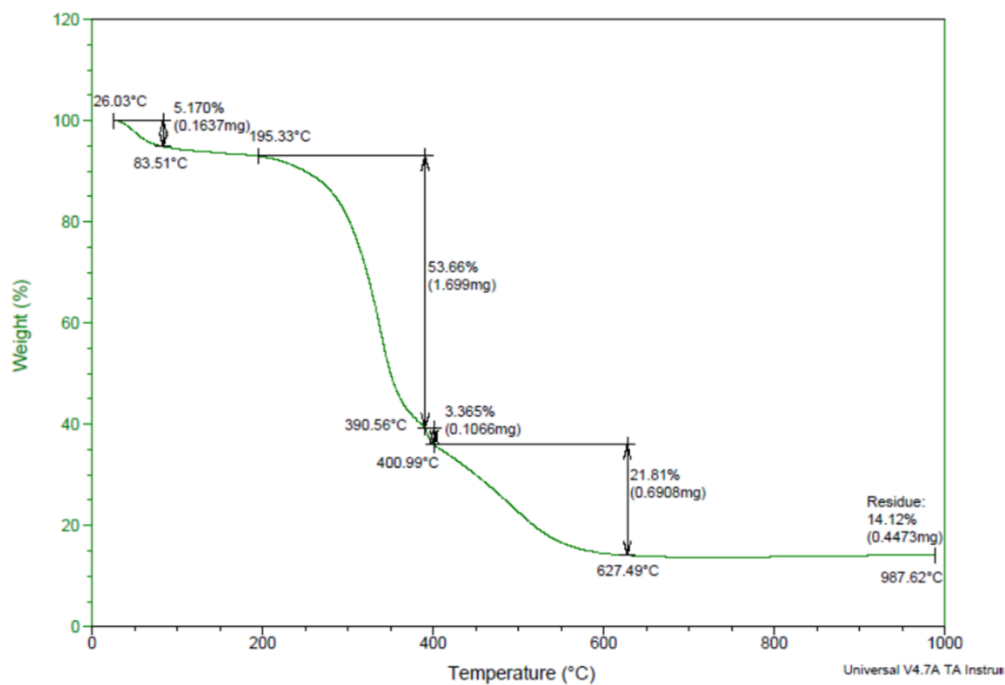


Fig. 2. Thermogravimetric analysis (TGA) curve of [CellImi]PF₆ (**11**)

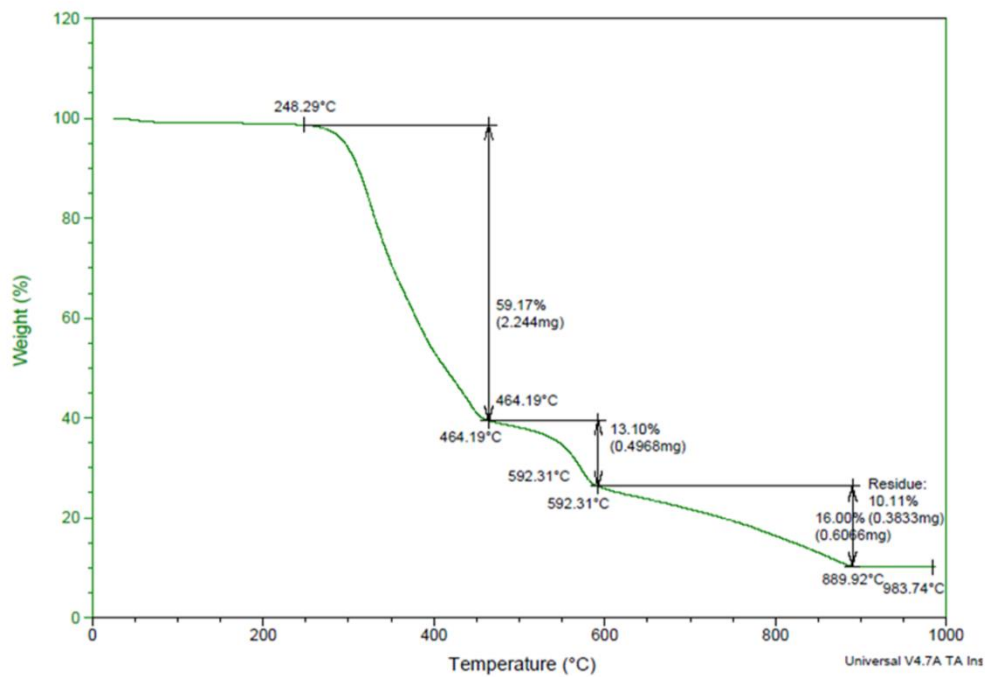


Fig. 3. Thermogravimetric analysis (TGA) curve of [MerImi]PF₆ (**14**)

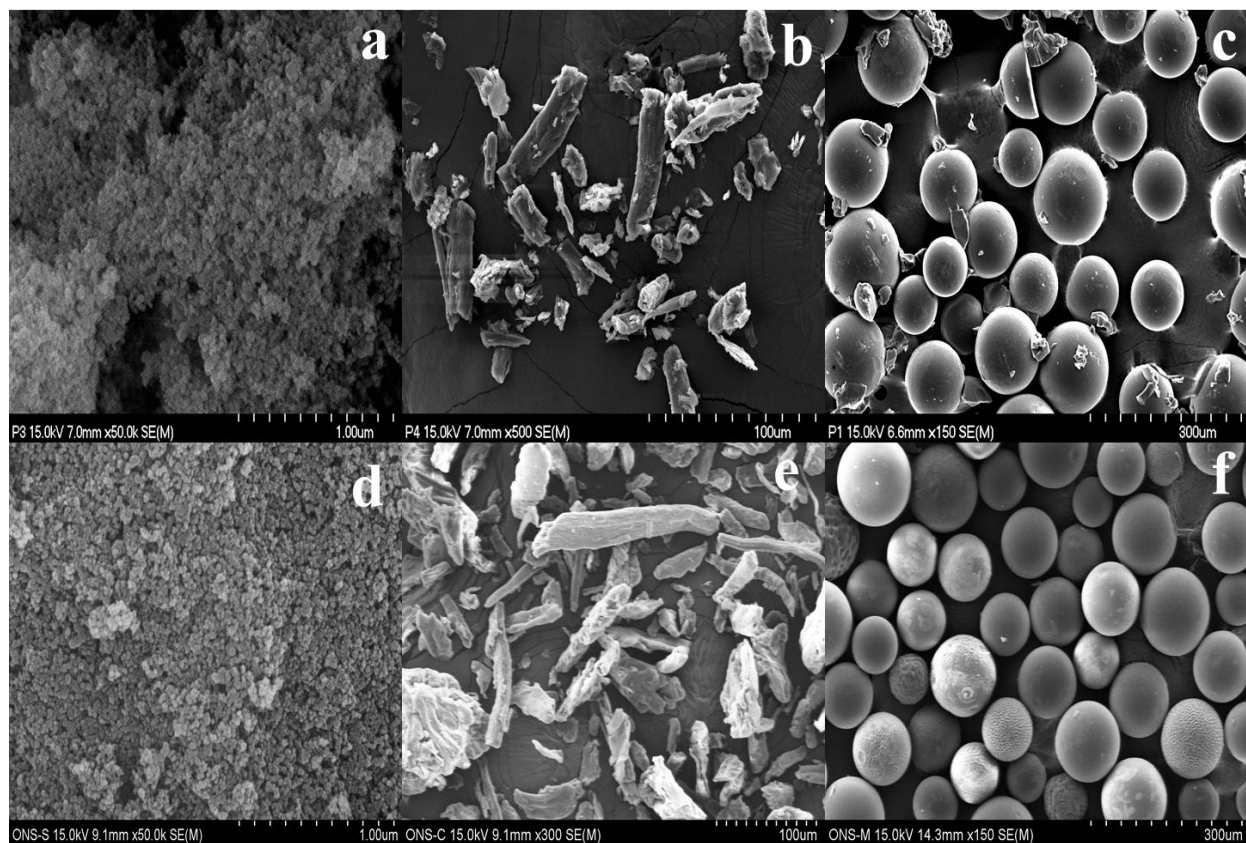


Fig. 4. FE-SEM images of (a) [SiIImi]PF₆ (**6**); (b) [CellImi]PF₆ (**11**); (c) [MerImi]PF₆ (**14**); (d) Aerogel silica; (e) Cellulose; (f) Merrifield resin

The field emission scanning electron microscopy (FE-SEM) analysis of [SiIImi]PF₆ (**6**), [CellImi]PF₆ (**11**), [MerImi]PF₆ (**14**) and their corresponding supports (**1**, **7** and **12**) is exemplified in **Fig. 4**. FE-SEM image of **6** (**Fig. 4(a)**) display uniform arrangement of ultrafine microparticles similar to pristine silica. The particles of **11** (**Fig. 4(b)**) appear irregular in shape with micrometer size similar to pristine cellulose. Moreover, the Merrifield resin beads in **14** (**Fig. 4(c)**) did not appear spherical like original Merrifield resin. The bead degradation was observed which may be created due to grafting of IL like units [11].

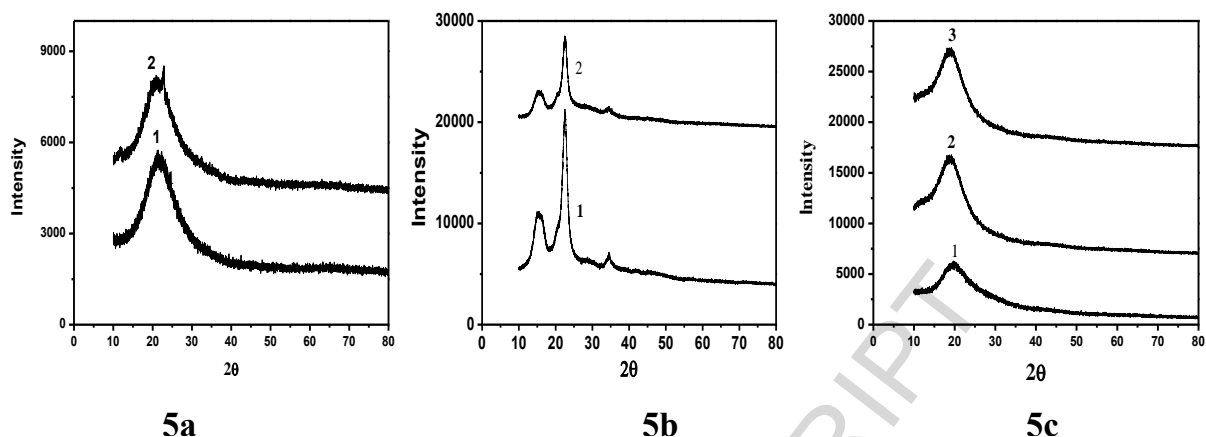
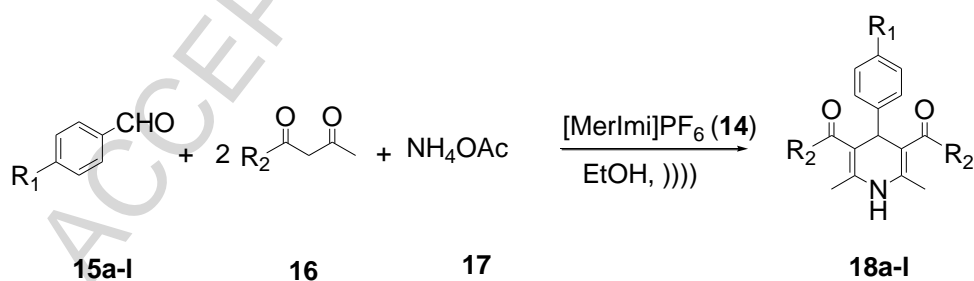


Fig. 5a: (1) XRD of [SilImi]Cl (**5**), (2) [SilImi]PF₆ (**6**); **5b:** (1) XRD of [CellImi]Cl (**10**), (2) [CellImi]PF₆ (**11**); **5c:** (1) XRD of [MerImi]Cl (**13**), (2) [MerImi]PF₆ (**14**), (3) Reused [MerImi]PF₆ (**14**)

X-ray diffraction (XRD) patterns of [SilImi]PF₆ (**6**), [CellImi]PF₆ (**11**), [MerImi]PF₆ (**14**) are demonstrated in **Fig. 5** and reveal strong diffraction peaks centred at angle $2\theta = 22^\circ$ for silica [12a], 16° , 22° , 34° for cellulose [12b], 19° for polystyrene [12c] signifying that the structural integrity of basic support material is retained in SILP catalysts [12c]. Moreover, absence of any characteristic reflection of hexafluorophosphate anion in the XRD patterns of **6**, **11**, **14** suggests uniform distribution of PF₆ anions in the SILP catalysts.

The catalytic efficiency of [SilImi]PF₆ (**6**), [CellImi]PF₆ (**11**), [MerImi]PF₆ (**14**) was screened in the synthesis of 1,4-Dihydropyridines (1,4-DHPs) (Scheme 2), which are privileged scaffolds in medicinal chemistry with diverse pharmacological and therapeutical properties. Many of their derivatives exhibited anticancer [13a], antidiabetic [13b-c], anti-inflammatory [13d] and photosensitizing activity [13e]. Due to their fascinating structural features these are employed as anti-HIV protease inhibitor [13f], neuroprotective agents [13g] and also, these are frequently used in the treatment of Alzheimer's disease [13h], cardiovascular disease [13i]. Potential of several 1,4-DHPs has been explored in clinically significant drugs such as

nifedipine, amlodipine, felodipine, nicardipine, nitrendipine, nislodipine and nimodipine [13j]. Due to diverse pharmacological properties, a plethora of distinct synthetic methodologies have been reported for synthesis of 1,4-DHPs which include bis-cinchona mediated reaction of malanonitrile and enamine derivatives [14a], reaction of *N,N*-dimethyl enamines and amines by oxidative mode [14b], iodine catalyzed reaction of primary amine, dialkyl acetylene dicarboxylates, aldehyde and pyruvic acid [14c], copper (II) triflate mediated cyclizations of alkynes, amines and α,β -unsaturated aldehydes [14d], reaction of aldehyde, β -keto ester and different sources of ammonia employing variety of catalytic systems [15], reaction of diketene, primary amines, malononitrile with aldehydes [14e]. Amongst these, reaction of aldehyde, β -keto ester and different sources of ammonia represents most elegant protocol. A variety of catalytic systems has been reported to improve the efficiency of this protocol [15]. However, despite of impressive progress, there is still scope for improvement especially toward developing an energy efficient protocol using synergistic effect of ultrasound and SILP catalyts. This prompted us to evaluate catalytic activity of SILP catalyts ([SiIImi]PF₆ (**6**) / [CellImi]PF₆ (**11**) / [MerImi]PF₆ (**14**)) under ultrasound in the synthesis of 1,4-DHPs.

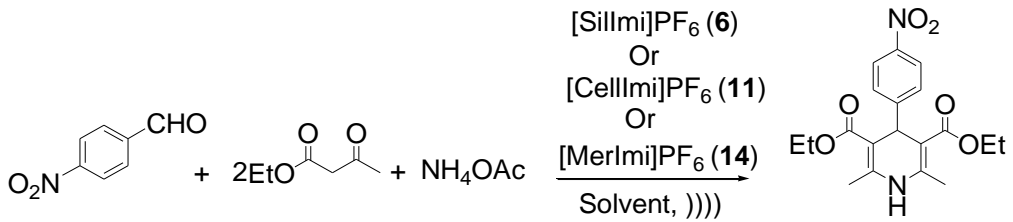


Scheme 2. Synthesis of 1,4-dihydropyridines from aldehyde, ethyl acetoacetate and ammonium acetate using [MerImi]PF₆ (**14**)

Initial studies to examine the effect of solvent and catalyst loading were carried out using model reaction between 4-nitrobenzaldehyde (**15a**), ethyl acetoacetate (**16**) and ammonium

acetate (**17**). We observed that catalyst loading had a profound influence on the course of reaction. When the amount of [SiIImi]PF₆ (**6**), [CellImi]PF₆ (**11**), [MerImi]PF₆ (**14**) was increased from 50 mg to 100 mg, the yield of corresponding product diethyl-2,6-dimethyl-4-(4-nitrophenyl)-1,4-dihydropyridine-3,5-dicarboxylate (**18a**) raised considerably (from 65% to 87% for **6**, 67% to 89% for **11**, 70% to 96% for **14**; Table 1, entries 3-4). However, further increase in the catalyst amount did not substantially improve yield of product (Table 1, entries 5-6).

In order to identify solvent of choice, a variety of solvents were screened. Evident from the basic screening process (Table 1), the reaction proceeds well in a polar protic solvents like water, methanol, and ethanol (Table 1, entries 1-6). The reaction afforded moderate yields in polar aprotic solvents such as DMSO, DMF, THF and CH₃CN (Table 1, entries 7-10). Eventually, it was found that the relatively lower yields were acquired in non-polar solvents such as dichloromethane, toluene, 1,4-dioxane, chloroform (Table 1, entries 11-14). Amongst all the screened solvents, ethanol was adopted as the solvent of choice because it led to a short reaction time and furnished maximum yield of anticipated product (Table 1, entries 3-6). The results of optimization study revealed that [MerImi]PF₆ (**14**) exhibited highest catalytic activity in the synthesis of 1,4-DHPs and hence it was used for further studies.

Table 1. Optimization of catalyst loading and solvent in synthesis of 1,4-dihydropyridines^a


Entry	Solvent	Amount of catalyst (mg)	Time (Min.) Support@PF ₆			Yield (%) ^b Support@PF ₆		
			[SilImi]PF ₆ (6)	[CellImi]PF ₆ (11)	[MeImi]PF ₆ (14)	(6)	(11)	(14)
1	H ₂ O	100 ^d	50	45	35	57	61	65
2	MeOH	100 ^d	35	30	25	81	85	87
3	EtOH	50 ^c	25	30	20	65	67	70
4	EtOH	100^d	20	15	10	87	89	96
5	EtOH	150 ^e	25	15	10	90	91	97
6	EtOH	200 ^f	25	15	10	90	91	97
7	DMSO	100 ^d	45	55	65	45	48	50
8	DMF	100 ^d	65	60	55	40	42	47
9	THF	100 ^d	75	70	65	38	40	45
10	CH ₃ CN	100 ^d	60	50	40	37	39	49
11	CH ₂ Cl ₂	100 ^d	65	55	55	25	25	35
12	Toluene	100 ^d	72	70	61	15	20	25
13	1,4-dioxane	100 ^d	55	45	35	10	15	10
14	CHCl ₃	100 ^d	77	75	70	25	27	30

^a Reaction conditions: 4-Nitrobenzaldehyde (1.0 mmol), ethyl acetoacetate (2.0 mmol), ammonium acetate (1.0 mmol), solvent (5 mL). ^b Isolated yields after chromatography. ^c % Loading of catalyst per 50 mg: (0.020 mmol of [SilImi]PF₆), (0.027 mmol of [CellImi]PF₆), (0.032 mmol of [MerImi]PF₆). ^d % Loading of catalyst per 100 mg: (0.040 mmol of [SilImi]PF₆), (0.054 mmol of [CellImi]PF₆), (0.064 mmol of [MerImi]PF₆). ^e % Loading of catalyst per 150 mg: (0.060 mmol of [SilImi]PF₆), (0.081 mmol of [CellImi]PF₆), (0.096 mmol of [MerImi]PF₆). ^f % Loading of catalyst per 200 mg: (0.080 mmol of [SilImi]PF₆), (0.108 mmol of [CellImi]PF₆), (0.128 mmol of [MerImi]PF₆).

With the optimized reaction conditions in hand, we probed the general applicability of protocol by reacting variety of aromatic aldehydes **15** (1.0 mmol) with ethyl acetoacetate **16** (2.0 mmol) and ammonium acetate **17** (1.0 mmol) in the presence of **14** (100 mg) in ethanol (5 mL) under ultrasonic irradiation at room temperature for synthesis of library of 1,4-DHPs. The

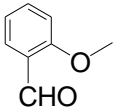
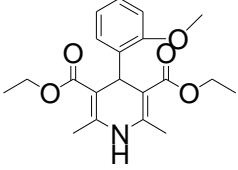
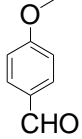
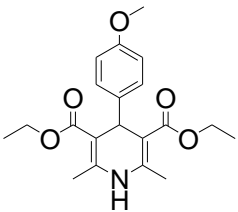
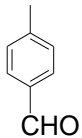
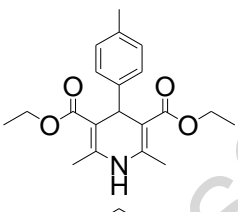
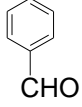
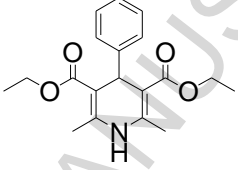
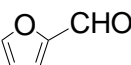
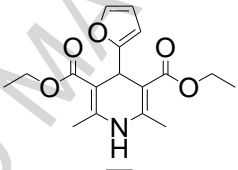
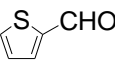
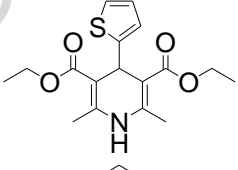
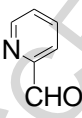
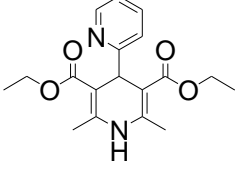
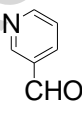
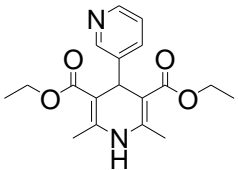
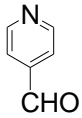
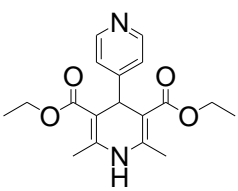
reactions proceeded efficiently forming the desired products in high yields within short time and the results were summarized in Table 2. Aldehydes with electron withdrawing group (Table 2, entries **15a,c**) furnished the higher yields than aldehydes bearing electron donating group (Table 2, entries **15e-f**). Sterically hindered aldehydes (Table 2, entries **15b,d**) such as *o*-nitrobenzaldehyde and *o*-anisaldehyde also performed well affording moderate yields of the anticipated products. Heteroaromatic aldehydes such as 2-furaldehyde, 2-thiophenecarboxaldehyde, pyridin-2-aldehyde, pyridin-3-aldehyde and pyridin-4-aldehyde reacted efficiently forming the anticipated products in good yields (Table 2, entries **15h-l**).

Table 2. [MerImi]PF₆ (**14**) catalyzed synthesis of 1,4-dihydropyridines^a

$$\text{R}_1\text{-C}_6\text{H}_4\text{-CHO} + 2 \text{R}_2\text{-C(=O)-CH}_2\text{-C(=O)-R}_2 + \text{NH}_4\text{OAc} \xrightarrow[\text{EtOH, } \text{)}\text{)}]{[\text{MerImi}]\text{PF}_6 \text{ (14)}} \text{R}_1\text{-C}_6\text{H}_3\text{(R}_2)_2\text{-NHC(=O)R}_2$$

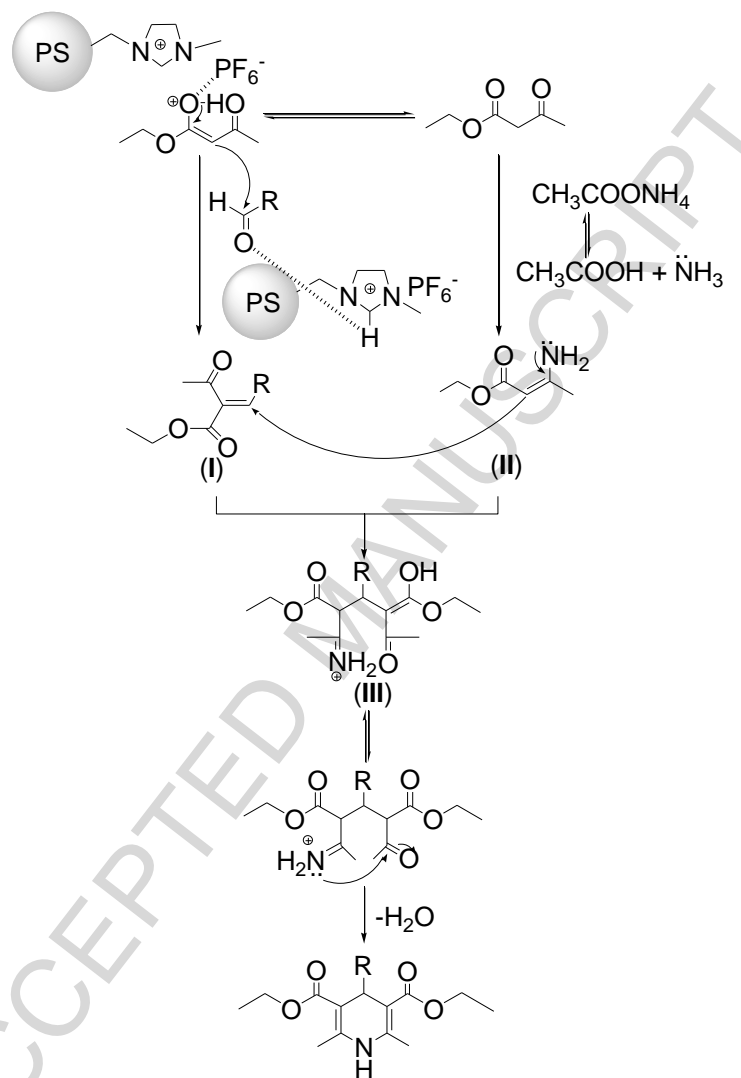
15a-l **16** **17** **18a-l**

Entry	Aldehyde (15)	Product (18)	Time (min.)	Yield ^b (%)
a			10	96
b			12	87
c			10	94

d			20	79
e			15	90
f			15	89
g			10	87
h			20	90
i			22	86
j			25	85
k			15	86
l			18	89

^a Reaction conditions: Aldehyde (1.0 mmol), ethyl acetoacetate (2.0 mmol), ammonium acetate (1.0 mmol), ethanol (5 mL), [MerImi]PF₆ (100 mg); ^b Isolated yields after chromatography.

The identity of all the compounds was ascertained on the basis of IR, ^1H NMR, ^{13}C NMR and mass spectroscopy. The physical and spectroscopic data are in harmony with the proposed structures and are in well agreement with the literature data.



Scheme 3. A plausible mechanism for [MerImi]PF₆ (**14**) mediated synthesis of 1,4-dihydropyridines

A plausible mechanism for [MerImi]PF₆ (**14**) catalyzed synthesis of 1,4-DHPs is depicted in **Scheme 3**. Initially, PF₆ anion coordinates with enolic form of ethyl acetoacetate [16a]. Further, the hydrogen bond bonding ability of C₂-H of imidazolium ring activates carbonyl group

of aldehyde [16b]. This facilitates Knoevenagel condensation between 1,3-dicarbonyl compound and aryl aldehydes yielding α,β -unsaturated carbonyl compound (**I**). Further, the enamine intermediate (**II**) that is formed initially by reaction of 1,3-dicarbonyl compound with ammonia undergo Michael addition with **I** yielding **III**. Lastly, the subsequent cyclization following by dehydration results into formation of 1,4-DHPs.

To determine whether the $[\text{MerImi}]\text{PF}_6$ (**14**) is really heterogeneous, we performed a split test using a model reaction. While performing such a test, **14** was filtered off after 50% of the reaction was completed (GC-MS analysis) and the liquid phase of the reaction mixture was sonicated at room temperature for additional time. Interestingly, no considerable progress (GC-MS analysis) was observed.

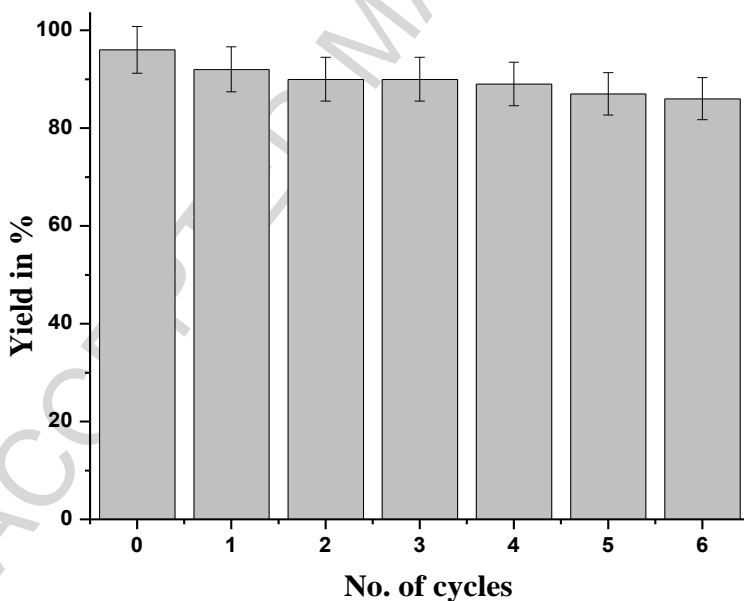


Fig.6. Reusability of $[\text{MerImi}]\text{PF}_6$ (**14**) in 1,4-dihydropyridine synthesis

The recyclability of $[\text{MerImi}]\text{PF}_6$ (**14**) was accessed by employing the model reaction for synthesis of **18a**. In brief, after each cycle the catalyst was filtered and washed with ethanol and dried in vacuo indicate that the reaction occurs under heterogeneous condition. Following this

procedure, the recovered catalyst was reused for six times as illustrated in **Fig. 6**. The studies revealed minimal loss in catalytic activity on successive cycles under optimized reaction conditions.

Impact of ultrasound on the chemical, physical nature and stability of [MerImi]PF₆ (**14**) has been studied with help of FT-Raman, FT-IR and CP-MAS ¹³C NMR spectroscopy as well as XRD, SEM, EDX and TGA analysis. The FT-Raman analysis of reused **14** displayed the characteristic peaks due to out-plane C-H bending vibration of imidazolium ring (782 cm⁻¹), in-plane wagging vibration of alkyl chain (1080 cm⁻¹), symmetrical stretching vibration of alkyl chain (2903 cm⁻¹) and the symmetric P-F stretching of PF₆ anion (739 cm⁻¹). FT-Raman analysis revealed that fresh and reused catalysts have the same patterns, indicating that reused **14** was stable even after ultrasonic irradiation. The FT-IR spectrum of reused **14** exhibited in-plane C-H deformation (1446 cm⁻¹), in-plane C-N stretching vibration of imidazolium ring (1599 cm⁻¹) and aliphatic C-H stretching vibration (2913 cm⁻¹). The characteristic peak of P-F stretching of PF₆ anion was observed at 820 cm⁻¹, which is convincing evidence for the fact that functional groups present in pristine **14** is retained in the reused catalyst even after recycling. CP-MAS ¹³C NMR spectrum of reused **14** demonstrated the peaks at 41.0 (-CH₃ of imidazolium ring), 53.4 (-CH₂ group between imidazolium and benzene ring), 128.7, 138.0, 146.4 (imidazolium Cs), 120-146 (peaks due to C atoms of aromatic polystyrene framework overlapped with peaks of imidazolium Cs) and which is similar to the pristine **14**.

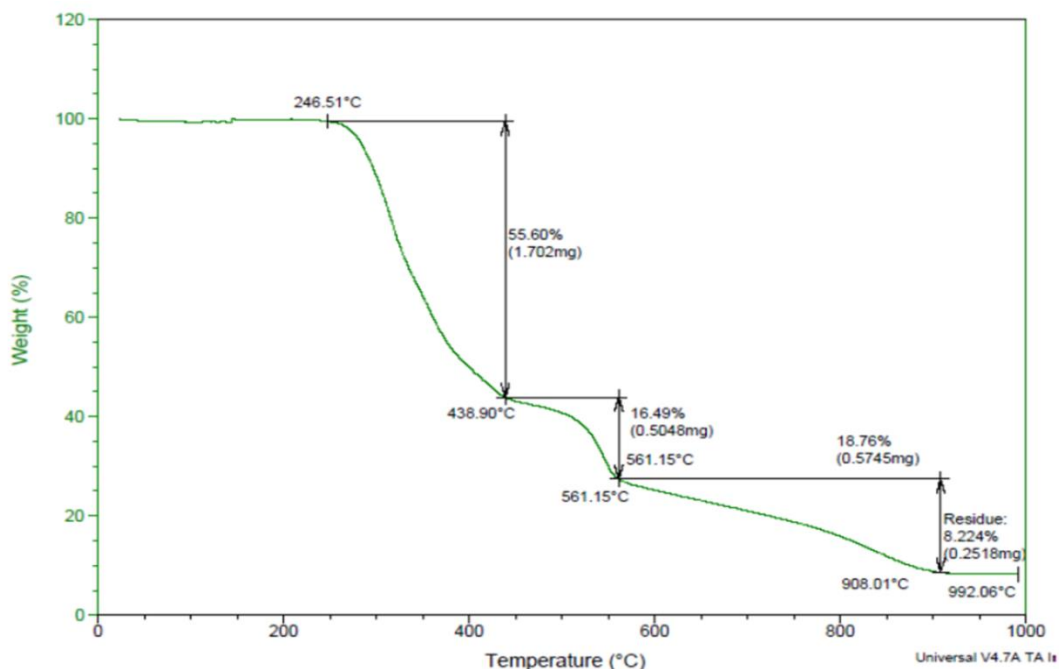


Fig. 7. Thermogravimetric analysis (TGA) curve of reused [MerImi]PF₆ (**14**)

XRD pattern of reused [MerImi]PF₆ (**14**) mimicked the XRD pattern of pristine **14** (**Fig. 5c**). The EDX analysis of reused **14** revealed that there was no significant alteration in composition of pristine and reused **14**. The TGA analysis of reused **14** is shown in **Fig. 7**. TGA thermogram exhibited an initial weight loss of 55.60% (246 °C to 438 °C) due to decomposition of organic moieties confined on Merrifield resin and loss of IL like unit. Consecutive weight loss of 16.49% (438 °C to 561 °C) is ascribed to decomposition of Merrifield resin backbone. Finally residual weights correspond to the formation of carbonates due to incomplete combustion of polymeric material or generation of carbonaceous matter. The FE-SEM analysis of reused **14** (**Fig. 8**) revealed that the morphology of catalyst is preserved even after reuse. These results reveal that structural rigidity of **14** is conserved even after reuse, confirming that SILP catalysts do not undergo physical and chemical changes under ultrasonic irradiation.

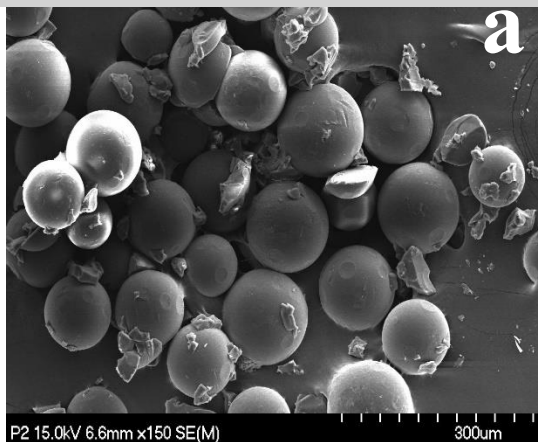


Fig. 8. FE-SEM image of (a) reused [MerImi]PF₆ (14)

4. Conclusion

In conclusion, we have investigated the compatibility of Merrifield resin, silica and cellulose supported ionic liquid phase catalysts in the synthesis of bioactive 1,4-dihydropyridines under ultrasonic irradiation. The impact of ultrasonication on the properties of SILP catalysts was evaluated using various analytical techniques. The FT-Raman, FT-IR, CP-MAS ¹³C NMR analysis of reused SILP catalysts displayed the characteristic peaks similar to fresh SILP catalysts. The XRD and TGA patterns of reused catalysts mimicked with fresh SILP catalysts. The EDX analysis of reused SILP catalysts did not show that substantial alteration in composition of fresh and reused SILP catalysts. The FE-SEM analysis of reused SILP catalysts revealed that the morphology is conserved even after continuous reuse. The results reveal that sonication of SILP catalysts does not lead to physical, chemical and structural changes unlike traditional ILs confirming that SILP catalysts are stable even after ultrasonic irradiation. The synergistic effect of ultrasound and SILP catalysts is likely to emerge as promising research avenue worth broad interest for development in future.

Acknowledgements

The author is deeply grateful to Indian Institute of Sciences (IISc), Bangalore and Sophisticated Analytical Instrumental Facility, Indian Institute of Technology, Madras (IITM) for providing

spectral facilities and Shivaji University Kolhapur for providing Departmental Research Fellowship.

References

1. (a) J.S. Ghomi, S. Zahedi, Novel ionic liquid supported on Fe₃O₄ nanoparticles and its application as a catalyst in Mannich reaction under ultrasonic irradiation, *Ultrason. Sonochem.* 34 (2017) 916-923; (b) M. Zakeri, M.M. Nasef, E. Abouzari-Lotf, Eco-safe and expeditious approaches for synthesis of quinazoline and pyrimidine-2-amine derivatives using ionic liquids aided with ultrasound or microwave irradiation, *J. Mol. Liq.* 199 (2014) 267–274; (c) S. Rostamnia, H. Xin, Simultaneous application of ultrasonic irradiation and immobilized ionic liquid onto the SBA-15 nanoreactor (US/[MPIm]Cl@SBA-15): A robust, recyclable, and useful combined catalytic system for selective and waste-free Kabachnik Fields reaction, *J. Mol. Liq.* 195 (2014) 30–34; (d) B.R. Raju, D.M.F. Sampaio, M.M. Silva, P.J.G. Coutinho, M.S.T. Goncalves, Ultrasound promoted synthesis of Nile Blue derivatives, *Ultrason. Sonochem.* 21 (2014) 360-366.
2. (a) V. Kumar, A. Sharma, M. Sharma, U.K. Sharma, A.K. Sinha, DDQ catalyzed benzylic acetoxylation of arylalkanes: a case of exquisitely controlled oxidation under sonochemical activation, *Tetrahedron* 63 (2007) 9718-9723; (b) R.S. Varma, Greener and Sustainable Trends in Synthesis of Organics and Nanomaterials, *ACS Sustain. Chem. Eng.* 4 (2016) 5866-5878; (c) G. Cravotto, P. Cintas, Power ultrasound in organic synthesis: moving cavitation chemistry from academia to innovative and large-scale applications, *Chem. Soc. Rev.* 35 (2006) 180-196; (d) M. Sillanpaa, T.–D. Pham, R.A.

- Shrestha, *Ultrasound Technology in Green Chemistry*, Springer, Netherlands, 2011, pp. 1–21.
3. (a) N.C. Eddingsaas, K.S. Suslick, *Mechanoluminescence: light from sonication of crystal slurries*, *Nature* 444 (2006) 163; (b) M. Ashokkumar, *The characterization of acoustic cavitation bubbles - an overview*, *Ultrason. Sonochem.* 18 (2011) 864-872; (c) S. Merouani, H. Ferkous, O. Hamdaoui, Y. Rezgui, M. Guemini, *Ultrason. Sonochem.* 22 (2015) 51-58; (d) P. Cintas, *On Cavitation and Chirality: A Further Assessment*, *Cryst. Growth Des.* 8 (2008) 2626-2627.
 4. (a) G. Chatel, D.R. MacFarlane, *Ionic liquids and ultrasound in combination: synergies and challenges*, *Chem. Soc. Rev.* 43 (2014) 8132-8149; (b) J.D. Oxley, T. Prozorov, K.S. Suslick, *Sonochemistry and Sonoluminescence of Room-Temperature Ionic Liquids*, *J. Am. Chem. Soc.* 125 (2003) 11138-11139; (c) G. Chatel, R. Pflieger, E. Naffrechoux, S.I. Nikitenko, J. Suptil, C. Goux-Henry, N. Kardos, B. Andrioletti, M. Draye, *Hydrophobic Bis(trifluoromethylsulfonyl)imide-Based Ionic Liquids Pyrolysis: Through the Window of the Ultrasonic Reactor*, *ACS Sustainable Chem. Eng.* 1 (2013) 137-143; (d) D.J. Flannigan, S.D. Hopkins, K.S. Suslick, *Sonochemistry and sonoluminescence in ionic liquids, molten salts, and concentrated electrolyte solutions*, *J. Organomet. Chem.* 690 (2005) 3513-3517; (e) P.M. Kanthale, M. Ashokkumar, F. Grieser, *Estimation of Cavitation Bubble Temperatures in an Ionic Liquid*, *J. Phys. Chem. C* 111 (2007) 18461-18463.
 5. A.R. Gholap, K. Venkatesan, T. Daniel, R.J. Lahoti, K.V. Srinivasan, *Ionic liquid promoted novel and efficient one pot synthesis of 3,4-dihydropyrimidin-2-(1*H*)-ones at ambient temperature under ultrasound irradiation*, *Green Chem.* 6 (2004) 147-150.

6. (a) D.G. Hanna, S. Shylesh, S. Werner, A.T. Bell, The kinetics of gas-phase propene hydroformylation over a supported ionic liquid-phase (SILP) rhodium catalyst, *J. Catal.* 292 (2012) 166-172.
7. (a) C.P. Mehnert, R.A. Cook, N.C. Dispenziere, M. Afeworki, Supported ionic liquid catalysis-a new concept for homogeneous hydroformylation catalysis, *J. Am. Chem. Soc.* 124 (2002) 12932-12933; (b) A. Riisagar, R. Fehrmann, M. Haumann, P. Wasserscheid, Supported Ionic Liquid Phase (SILP) Catalysis: An Innovative Concept for Homogeneous Catalysis in Continuous Fixed-Bed Reactors, *Eur. J. Inorg. Chem.* (2006) 695-706.
8. R. Kurane, J. Jadhav, S. Khanpure, R. Salunkhe, G. Rashinkar, Synergistic catalysis by an aerogel supported ionic liquid phase (ASILP) in the synthesis of 1,5-benzodiazepines, *Green Chem.* 15 (2013) 1849-1856.
9. (a) H. Li, P.S. Bhadury, B. Song, S. Yang, Immobilized functional ionic liquids: efficient, green, and reusable catalysts, *RSC Adv.* 2 (2012) 12525-12551; (b) R. Kurane, S. Khanpure, D. Kale, R. Salunkhe, G. Rashinkar, An expedient synthesis of oxazolones using a cellulose supported ionic liquid phase catalyst, *RSC Adv.* 6 (2016) 44135-44144; (c) M. Isabel Burguete, H. Erythropel, E. Garcia-Verdugo, S.V. Luis, V. Sans, Base supported ionic liquid-like phases as catalysts for the batch and continuous-flow Henry reaction, *Green Chem.* 10 (2008) 401-407; (d) S. Doherty, J.G. Knight, M.A. Carroll, A.R. Clemmet, J.R. Ellison, T. Backhouse, N. Holmes, L.A. Thompson, R.A. Bourne, Efficient and selective oxidation of sulfides in batch and continuous flow using styrene-based polymer immobilised ionic liquid phase supported peroxotungstates, *RSC Adv.* 6 (2016) 73118-73131; (e) B. Xin, J. Hao, Imidazolium-based ionic liquids grafted on solid surfaces, *Chem. Soc. Rev.* 43

- (2014) 7171-7187; (f) S. Demirci, N. Sahiner, PEI-based ionic liquid colloids for versatile use: Biomedical and environmental applications, *J. Mol Liq.* 194 (2014) 85–92; (g) N. Sahiner, S. Demirci, Natural microgranular cellulose as alternative catalyst to metal nanoparticles for H₂ production from NaBH₄ methanolysis, *Appl. Catal. B. Environ.* 202 (2017) 199-206; (h) N. Sahiner, A. Yasar, Imidazolium based polymeric ionic liquid microgels as an alternative catalyst to metal catalysts for H₂ generation from methanolysis of NaBH₄, *Fuel Process. Technol.* 152 (2016) 316–324; (i) S. Demirci, K. Sel, N. Sahiner, Ionic liquid colloids based on PEI for versatile use, *Sep. Purif. Technol.* 155 (2015) 66-74; (j) N. Sahiner, A. Yasar, A New Application for Colloidal Silica Particles: Natural, Environmentally Friendly, Low-Cost, and Reusable Catalyst Material for H₂ Production from NaBH₄ Methanolysis, *Ind. Eng. Chem. Res.* 55 (2016) 11245–11252.
10. (a) Y. Hu, Z.C. Chen, Z.G. Le, Q.G. Zheng, Organic Reactions in Ionic Liquids: Ionic Liquid Promoted Knoevenagel Condensation of Aromatic Aldehydes with (2-Thio)Barbituric Acid, *Synth. Commun.* 34 (2004) 4521-4529; (b) J.S. Yadav, B.V.S. Reddy, P.N. Reddy, M. Shesha Rao, Bi(OTf)₃-[Bmim]PF₆: A novel and Reusable Catalytic System for the Synthesis of *cis*-Aziridine Carboxylates, *Synthesis* (2003) 1387-1389; (c) W. Sun, C.G. Xia, H.W. Wang, Synthesis of aziridines from imines and ethyl diazoacetate in room temperature ionic liquids, *Tetrahedron Lett.* 44 (2003) 2409-2411; (d) K.V. Wagh, B.M. Bhanage, Amberlyst-15/[Bmim][PF₆] Catalyzed Synthesis of C₃-Symmetric Triarylbenzenes via Cyclotrimerization of Alkynes, *ACS Sustain. Chem. Eng.* 4 (2016) 4232-4236; (e) M.K. Potdar, M.S. Rasalkar, S.S. Mohile, M.M. Salunkhe,

- Convenient and efficient protocols for coumarin synthesis via Pechmann condensation in neutral ionic liquids, *J. Mol. Catal. A: Chem.* 235 (2005) 249-252.
11. G. Rashinkar, R. Salunkhe, Ferrocene labelled supported ionic liquid phase (SILP) containing organocatalytic anion for multi-component synthesis, *J. Mol. Catal. A: Chem.* 316 (2010) 146-152.
 12. (a) M. Jagadale, S. Khanapure, R. Salunkhe, M. Rajmane, G. Rashinkar, Sustainable synthesis of sulfonamides using supported ionic liquid phase catalyst containing Keggin-type anion, *Appl. Organometal. Chem.* 30 (2016) 125-131; (b) S.M.K. Mohamed, K. Ganesan, B. Milow, L. Ratke, The effect of zinc oxide (ZnO) addition on the physical and morphological properties of cellulose aerogel beads, *RSC Adv.* 5 (2015) 90193-90201; (c) A.H. Jadhav, G.M. Thorat, K. Lee, A.C. Lim, H. Kang, J.G. Seo, Effect of anion type of imidazolium based polymer supported ionic liquids on the solvent free synthesis of cycloaddition of CO₂ into epoxide, *Catal. Today* 265 (2016) 56-67.
 13. (a) D.M. Stout, A.I. Meyers, Recent advances in the chemistry of dihydropyridines, *Chem. Rev.* 82 (1982) 223-243; (b) A.K. Ogawa, C.A. Willoughby, B. Raynald, K.P. Ellsworth, W.M. Geissler, R.W. Myer, J. Yao, H. Georgianna, K.T. Chapman, Glucose-lowering in a db/db mouse model by dihydropyridine diacid glycogen phosphorylase inhibitors, *Bioorg. Med. Chem. Lett.* 1 (2003) 3405-3408; (c) J.G. McCormack, N. Westergaard, M. Kristiansen, C.L. Brand, J. Lau, Pharmacological approaches to inhibit endogenous glucose production as a means of anti-diabetic therapy, *Curr. Pharm. Des.* 7 (2001) 1451-1474; (d) V.M. Briukhanov, I.F. Zverev, V.I. Elkin, The effect of calcium antagonists on the development of inflammatory effect in rat (in Russian), *Exp. Clin. Pharmacol.* 57 (1994) 47-49; (e) M. Martin-Caraballo, C.R. Triggle, D. Bieger,

- Photosensitization of oesophageal smooth muscle by 3-NO₂-1, 4-dihydropyridines: evidence for two cyclic GMP-dependent effector pathways, *Br. J. Pharmacol.* 116 (1995) 3293-3301; (f) C.K. Chu, V.S. Bhadti, K.J. Doshi, J.T. Etse, J.M. Gallo, F.D. Boudinot, R.F. Schinazi, Brain targeting of anti-HIV nucleosides: synthesis and in vitro and in vivo studies of dihydropyridine derivatives of 3'-azido-2',3'-dideoxyuridine and 3'-azido-3'-deoxythymidine, *J. Med. Chem.* 33 (1990) 2188-2192; (g) V. Klusa, Cerebrocrast. Neuroprotectant, cognition enhancer, *Drugs Future* 20 (1995) 135-138; (h) A. Hantzsch, Ueber die Synthese pyridinartiger Verbindungen aus Acetessigäther und Aldehydammoniak, *Justus Liebigs Ann. Chem.* 215 (1882) 1-82; (i) S.A. Khedkar, P.B. Auti, 1, 4-Dihydropyridines: a class of pharmacologically important molecules, *Mini. Rev. Med. Chem.* 14 (2014) 282-290; (j) A.B. Baranda, R.M. Alonso, R.M. Jimenez, W. Weinmann, Instability of calcium channel antagonists during sample preparation for LC–MS–MS analysis of serum samples, *Forensic Sci. Int.* 156 (2006) 23-34.
14. (a) F. Auria-Luna, E. Marques-Lopez, M. C. Gimeno, R. Heiran, S. Mohammadi, R.P. Herrera, Asymmetric Organocatalytic Synthesis of Substituted Chiral 1,4-Dihydropyridine Derivatives, *J. Org. Chem.* 82 (2017) 5516-5523; (b) F.C. Yu, B. Zhou, H. Xu, K.J. Chang, Y. Shen, An atom-economic green approach: oxidative synthesis of functionalized 1,4-dihydropyridines from *N,N*-dimethylenaminones and amines, *Tetrahedron Lett.* 56 (2015) 837-841; (c) A. Rezvanian, An expedient synthesis strategy to the 1,4-dihydropyridines and pyrido[1,2-*a*]quinoxalines: iodine catalyzed one-pot four-component domino reactions, *Tetrahedron* 72 (2016) 6428-6435; (d) S. Li, Q. Yang, J. Wang, Copper(II) triflate-catalyzed highly efficient synthesis of *N*-substituted 1,4-dihydropyridine derivatives via three-component cyclizations of alkynes, amines, and

- α,β -unsaturated aldehydes, *Tetrahedron Lett.* 57 (2016) 4500-4504; (e) A. Rezvanian, M. M. Heravi, Z. Shaabani, M. Tajbakhsh, Five-component synthesis of dihydropyridines based on diketene, *Tetrahedron* 73 (2017) 2009-2013.
15. (a) T.R. Ravikumar Naik, S.A. Shivashankar, Heterogeneous bimetallic ZnFe₂O₄ nanopowder catalyzed synthesis of Hantzsch 1,4-dihydropyridines in water, *Tetrahedron Lett.* 57 (2016) 4046-4049; (b) K. Azizi, J. Azarnia, M. Karimi, E. Yazdani, A. Heydari, Novel Magnetically Separable Sulfated Boric Acid Functionalized Nanoparticles for Hantzsch Ester Synthesis, *Synlett* 27 (2016) 1810-1813; (c) L.-Q. Kang, Z.-J. Cao, Z.-J. Lei, 2-Hydroxyethylammonium acetate: an efficient and reusable homogeneous catalyst for the synthesis of Hantzsch 1,4-dihydropyridines, *Montasch Chem.* 147 (2016) 1125-1128; (d) M. Yarhosseini, S. Javanshir, M.G. Dekamin, M. Farhadnia, Tetraethylammonium 2-(carbamoyl)benzoate as a bifunctional organocatalyst for one-pot synthesis of Hantzsch 1,4-dihydropyridine and polyhydroquinoline derivatives, *Monatsch Chem.* 147 (2016) 1779-1787; (e) J. Safari, F. Azizi, M. Sadeghi, Chitosan nanoparticles as a green and renewable catalyst in the synthesis of 1,4-dihydropyridine under solvent-free conditions, *New J. Chem.* 39 (2015) 1905-1909; (f) V.V. Srinivasan, M.P. Pachamuthu, R. Maheswari, Lewis acidic mesoporous Fe-TUD-1 as catalysts for synthesis of Hantzsch 1,4-dihydropyridine derivatives, *J. Porous Mater.* 22 (2015) 1187-1194; (g) H. Khabazzadeh, I. Sheikhshoae, S. Saeid-Nia, A molybdenum(VI) complex as an efficient catalyst for the synthesis of dihydropyridines, *Transition Met. Chem.* 35 (2010) 125-127; (h) G. Sabitha, K. Arundhathi, K. Sudhakar, B.S. Sastry, J.S. Yadav, CeCl₃·7H₂O-Catalyzed One-Pot Synthesis of Hantzsch 1,4-Dihydropyridines at Room Temperature, *Synth. Commun.* 39 (2009) 2843-2851; (i) K.L. Bridgwood, G.E. Veitch,

- S.V. Ley, Magnesium nitride as a convenient source of ammonia: preparation of dihydropyridines, *Org. Lett.* 10 (2008) 3627-3629; (j) A. Shaabani, A.H. Rezayan, A. Rahmati, M. Sharifi, Ultrasound-accelerated Synthesis of 1,4-Dihydropyridines in an Ionic Liquid, *Monatsh. Chem.* 137 (2006) 77-81.
16. (a) G. Angelini, C. Chiappe, P.D. Maria, A. Fontana, F. Gasparrini, D. Pieraccini, M. Pierini, G. Siani, Determination of the Polarities of Some Ionic Liquids Using 2-Nitrocyclohexanone as the Probe, *J. Org. Chem.* 70 (2005) 8193-8196; (b) L. Zhang, X. Fu, G. Gao, Anion-Cation Cooperative Catalysis by Ionic Liquids, *Chem. Cat. Chem.* 3 (2011) 1359-1364.

Highlights

► Structurally diverse supported ionic liquid phase catalysts containing hexafluorophosphate anion have been synthesized. ► Their catalytic activity is evaluated in synthesis of 1,4-dihydropyridines under ultrasonication. ► The study reveals that SILP catalysts do not undergo physical, chemical and structural changes under sonication.

ACCEPTED MANUSCRIPT